A Comparative Study of the Effects of Albedo Change on Drought in Semi-Arid Regions

JULE CHARNEY

Department of Meteorology, Massachusetts Institute of Technology, Cambridge 02139

WILLIAM J. QUIRK, SHU-HSIEN CHOW[1] AND JACK KORNFIELD[2]

NASA Institute for Space Studies, New York, N. Y. 10025

(Manuscript received 31 January 1977, in revised form 17 May 1977)

ABSTRACT

Results from a series of numerical simulations are presented to show the effects of changes in albedo on rainfall in six areas, two each in Africa, Asia and North America. Each pair consists of a semi-arid area lying at the boundary between a major desert and an adjacent monsoonal region, and an area of the same size located within the monsoonal region itself. The sensitivity of the rainfall to the ground hydrology was determined by performing the albedo simulations with two different evapotranspiration parameterizations, one giving too high evaporation over land and the other giving negligible evaporation over land. In the high evaporation case, an albedo change from 0.14 to 0.35 caused large decreases of rainfall in all three of the semi-arid test areas and in two of the three monsoonal test areas. In the negligible evaporation case the simulations were performed only for the three semi-arid areas; in this case the albedo increase produced a significant decrease in rainfall in only one of the areas, the Sahel. Intercomparison of the high and negligible evaporation cases shows that changes in evaporation rate are as important as changes in albedo. Thus, in all but one of the six areas local evaporation was a major factor in influencing rainfall.

When appreciable evaporation occurs, the mechanism by which an increase of albedo reduces the rainfall is as follows. Initially, the increase of albedo acts to reduce the absorption of solar radiation by the ground and therefore the transfer of sensible plus latent heat into the atmosphere. The resulting reduction in convective cloud tends to compensate for the increase of albedo by allowing more solar radiation to reach the ground, but it reduces the downward flux of longwave radiation even more, so that the *net* absorption of radiation by the ground, solar plus longwave, is decreased. Thus, with or without evaporation, the increase of albedo causes a net decrease of radiative flux into the ground and therefore a net decrease of convective cloud and precipitation.

1. Introduction

It is widely feared that man is inadvertently altering the delicate balance of the present climate (SMIC, 1971). This balance is especially precarious in the semi-arid zones bordering on the major deserts. Recently severe drought occurred in the Sahel at the southern margin of the Sahara when moist monsoon air failed to penetrate sufficiently far northward from the tropical Atlantic. Drought has been a recurrent problem in the provinces of India and Pakistan which border on the central Asiatic Deserts. In North America the highly productive lands of the western Great Plains lying just east of the Great Western Desert have suffered extended periods of drought, including the "dust-bowl" drought of the 1930's and the widespread drought of the 1950's. These regions have in common that large changes repeatedly take place in plant cover and ground hydrology and that maximum rainfall occurs during the summer monsoon season and is primarily convective in character.

In his Royal Meteorological Society Symons Memorial Lecture for 1974, Charney (1975) showed that the radiative heat loss caused by the high albedo of a desert contributes significantly to the sinking and drying of the air aloft and therefore to the reduction of precipitation. This dependence of precipitation on albedo led him to propose a biogeophysical feedback mechanism linking vegetation, albedo and precipitation as a partial explanation for recurrent drought in desert border areas. He suggested that if the soil is light, dry and sandy, as it often is in these areas, a decrease of vegetation will lead to an increase of albedo, a reduction of precipitation and therefore a further decrease in vegetation or at least a perpetuation of the initial decrease. This effect was

[1] Present affiliation: Computer Sciences Corporation, Silver Spring, Md. 20910.

[2] Present affiliation: Volcani Institute, POB 6, Bet Dagan, Israel.

expected to be further enhanced by the reduction in evapotranspiration resulting from the decrease in vegetation. In his view the vegetative cover at the border of a desert is to be regarded as unstable or metastable; if unstable, an initial departure from equilibrium will amplify; if metastable, it will at least tend to persist. The perturbation will remain until external counteracting climatological forces become large enough to overcome the local feedback effect and return the system toward the old equilibrium. These forces act to prevent still another possibility, namely, that if they did not exist or were sufficiently weak, the positive feedback could lead eventually to a new statistical equilibrium, i.e., to a new climate. Such a system would be intransitive in the sense defined by Lorenz (1968), having the property that different initial states lead to different climates. But if the external forces are sufficiently strong, the new statistical configuration cannot persist indefinitely, it can exist merely as a long-term perturbation of a basically stable statistical equilibrium.

Albedos can be changed by natural as well as anthropogenic factors. We do not distinguish between the two here, but if the entire system were being considered, in its biological and ecological as well as its geophysical aspects, a sharp distinction would have to be made, since anthropogenic changes involving changes in land use tend to be very persistent whereas natural ecosystems tend to recover more readily from natural perturbations.

In this article we present modeling evidence only for the reality of the geophysical, not the biological, component of the system. We show that the restoring climatological forces, consisting of the global circulations and their random perturbations, are too weak for the limited period of the integration to overcome or even mask the local effects of the albedo changes in the regions in question. Hence, whatever the ultimate behavior of the biogeophysical system as a whole, the feedback mechanism will exist and will have the effect of at least prolonging a given fluctuation, whether positive or negative, i.e., of prolonging both dry and rainy periods. Since drought is prolonged dryness, the postulated feedback mechanism can be expected to contribute to drought.

Control numerical integrations were carried out for the month of July with the general circulation model of the NASA Institute for Space Studies. These were repeated with surface albedos modified in certain selected regions: the Sahel, the western Great Plains and the semi-arid Rajputana area of southeastern Pakistan and northwestern India adjoining the very dry Thar or Indian Desert. For comparison purposes, a third integration was performed in which the albedos were altered simultaneously in central Africa, the Mississippi Valley and Bangladesh. These regions were selected as being rainier and more centrally imbedded in their respective monsoon regimes. Some early results for the Sahel integrations had already been presented by Charney *et al.* (1975, 1976).

Man-induced changes may very well have operated in the semi-arid zones dealt with in this article. In the western Great Plains, for example, erosion, agricultural tillage and crop harvesting have at times reduced the darker humus layer to expose the brighter lower horizons of the soil (Buckman and Brady, 1969). In the Sahel, there is strong evidence that overgrazing has caused surface albedos to increase over large areas (Otterman *et al.*, 1976) and as reported by Hora (1952), "the Rajputana Desert is largely a man-made desert . . . (formed) by the work of man in cutting down and burning forests . . . (and by) the deterioration of soils."

The last reference is taken from an article by Bryson and Baerreis (1967) who suggest that the dense pall of dust frequently found over northwestern India is a significant factor in increasing the infrared cooling of the air and thereby increasing its subsiding motion. Since destruction of vegetation destabilizes the soil and permits the wind to raise more dust, the possibility exists that the dust enhances our postulated biogeophysical feedback mechanism. However, dust also absorbs solar radiation, and it is not yet known whether it produces a net increase or decrease of radiative heating. Some early estimates suggest that the dust does not greatly change the planetary albedo but that it absorbs solar radiation in the mid-atmosphere and thereby reduces the heating of the ground (J. Hansen, personal communication, 1976). This effect would tend to stabilize the lower part of the atmosphere and inhibit thermal convection. It is not considered here.

Since accurate measurements of actual albedo changes on the earth have not yet been made, we have had to content ourselves with idealized numerical experiments with simplified albedo distributions and arbitrary albedo changes. To the extent that the albedo-induced perturbations are linear, their magnitudes can later be scaled for observed changes in albedo as these become available. The albedos for all permanent desert areas in the Northern Hemisphere were fixed at 0.35, and the albedos of the marginal and comparison areas were assigned the values 0.35 or 0.14; the albedos of all other land surfaces save permanent ice cover were taken to be 0.14; the ice albedo was assigned the value of 0.70, and the ocean surface albedo was taken to be 0.07. The albedos selected turn out to be within the range determined by Rockwood and Cox (1976) from satellite observations over northwestern Africa.

The locations of the permanent desert and marginal areas were assigned on the basis of relative regional brightness obtained from minimal planetary albedos (Rashke *et al.*, 1973). To insure computational sig-

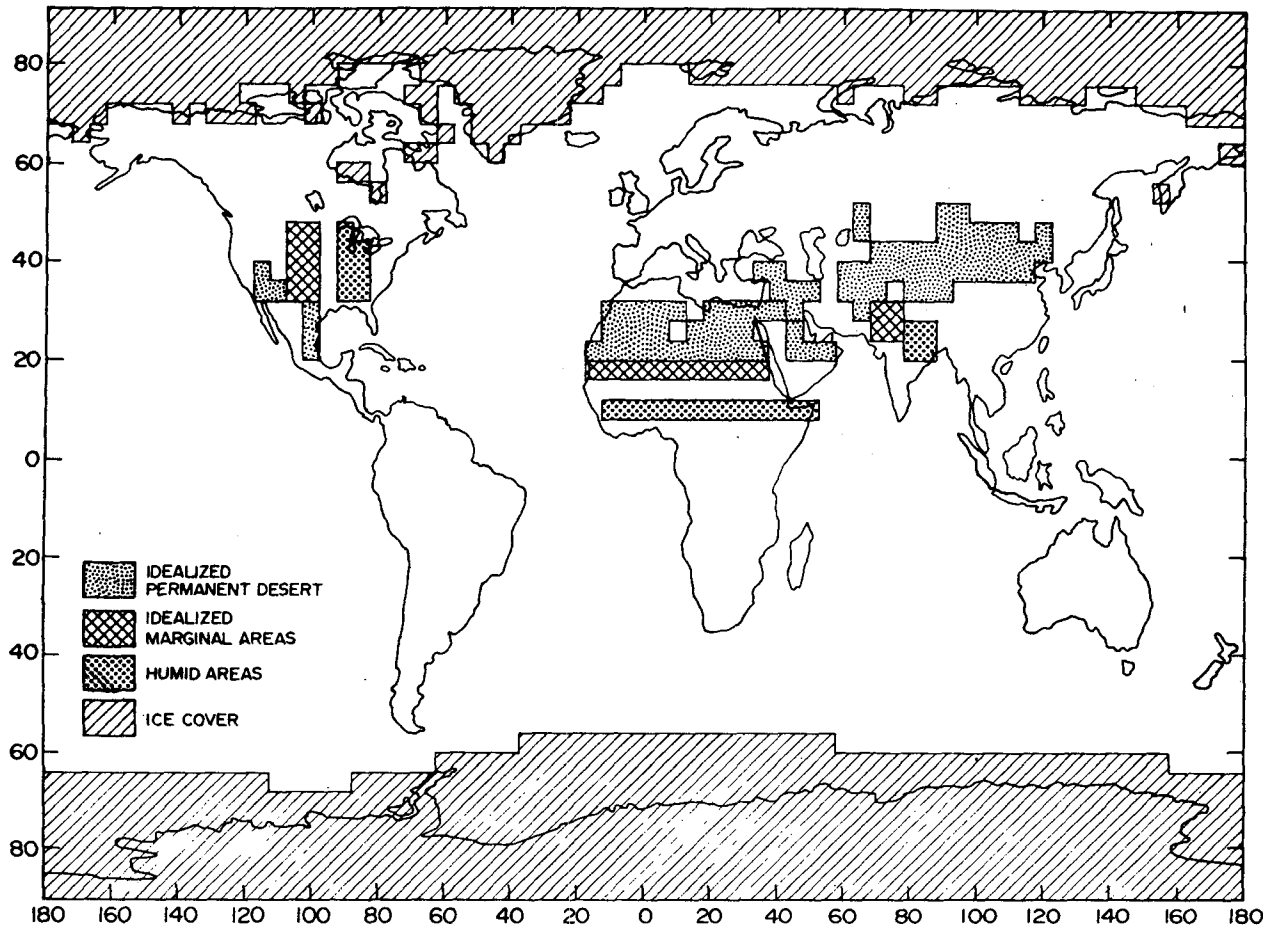

FIG. 1.1. Global albedo distribution assumed for experiments.

nificance the western Great Plains and Rajputana areas were made somewhat larger than they are in reality. Fig. 1.1 shows the albedo distributions assumed for the experiments.

2. The model

The numerical general circulation model employed for the studies was that of the Goddard Institute for Space Studies (GISS). It has been described by Somerville *et al.* (1974), and its July climatology for a land albedo of 0.14 has been discussed by Stone *et al.* (1977). The model contains two mechanisms for generating cloud and precipitation: 1) large-scale ascent leading to supersaturation, and 2) cumulus convection in conditionally unstable air. The cumulus convection parameterization is the same as that devised by Arakawa for the UCLA three-level model (Arakawa *et al.*, 1969). In the GISS nine-level model used for the experiments, the lower six levels were combined in pairs to produce three layers for the calculation of cumulus convection. Model convection occurred whenever a lower layer was buoyant with respect to a higher level. Convection stabilized the column, condensed water vapor, released latent heat and created clouds for input into the radiation portion of the model. Clouds arising from both types of condensation mechanisms were assumed to occupy an entire layer and to be black in the infrared. The effect of a cloud on solar radiation was made to depend on the cloud type, cloud depth and cloud height.

The hydrological parameterizations used in the model were exceedingly primitive. The ground wetness G, defined as the fraction of saturation of the soil, was fixed at values determined from mean July surface relative humidities (Stone *et al.*, 1977). The evaporation rate E was taken to be a fraction β of the potential evaporation rate P, the evaporation rate from saturated ground. In one set of integrations the coefficient β was set equal to the lesser of 1 or $2G$, as in the Arakawa model, but this assumption led to excessive evaporation over land. In a second set the empirical formula

$$\beta=\frac{1-\exp[44.6G/(1-0.99G)]}{\exp(0.87P)}$$

was introduced as being more typical of plant physio-

TABLE 3.1. Detailed description of six model runs discussed in the text.

Experiment no.	Numerical simulations Albedo Land	Ocean	Ice and snow	Desert*	Marginal**	Humid***	Evaporation over land
1	0.14	0.07	0.7	0.14	0.14	0.14	Excessive
2a	0.14	0.07	0.7	0.35	0.14	0.14	Excessive
2b	0.14	0.07	0.7	0.35	0.14	0.14	Negligible
3a	0.14	0.07	0.7	0.35	0.35	0.14	Excessive
3b	0.14	0.07	0.7	0.35	0.35	0.14	Negligible
4	0.14	0.07	0.7	0.35	0.14	0.35	Excessive

* Desert: Sahara, Nevada, Sonora, Gobi, etc. (see Fig. 1.1).
** Marginal: Sahel, Western Great Plains, Rajputana (see Fig. 1.1).
*** Humid: Bangladesh, Central Africa, Mississippi Valley (see Fig. 1.1).

logical characteristics. Unfortunately, the model considerably overestimated P and thus greatly reduced the values of E, so much so that the evaporation over land became nearly zero. Pending the completion of a more realistic model of evapotranspiration, which takes into account the variable storage of moisture in the ground and the ability of plants to enhance evaporation by drawing upon deeper lying moisture, it has been decided to present the results from the two primitive hydrologies as at least bracketing the effect of evaporation over land. The calculations with the excessive evaporation hydrology will be referred to as "excessive" or "high" evaporation experiments and those with the negligible evaporation hydrology as "negligible" or "low" evaporation experiments.

3. Model climatology for July

The actual state of the atmosphere on 18 June 1973, determined from data supplied by the National Meteorological Center, was taken as the initial state for the global integrations. The integrations were carried out for the six-week period (18 June–31 July). The sea-surface temperature and ice cover, as well as soil moisture, were fixed at their mean climatological values for July throughout the integration. The solar declination, solar insolation and snow lines were allowed to vary with time. The distributions of soil moisture, sea-surface temperature and ice cover are described in Stone *et al.* (1977). The parameters used in the various numerical experiments and their geophysical distributions are listed in Tables 3.1 and 3.2. By model "climatology" for July we mean merely an average for the month of July. The "climatology" described by Stone *et al.* corresponds to the first experiment in Table 3.1, in which the albedo over ice-free land was everywhere 0.14 and the excessive evaporation model hydrology was employed.

The assumption made here and throughout this article is that the calculated mean conditions for July are in fact a reasonable approximation to the model climatology for July. Thus when the integrations were extended two weeks into August for Experiments 1 and 2a, no significant changes were observed in the mean conditions. But a true statistical equilibrium would require numerical calculations for many model years. And it would not suffice to keep the sun fixed in the heavens because the atmosphere-earth system has relaxation times which are long compared to a month, as for example for water storage in the ground or heat storage in the upper mixed layer of the oceans.

a. Influence of albedo on rainfall and evaporation in the Northern Hemisphere

The simulated precipitation rates for the first and third experiments are compared with observations in Figs. 3.1. A comparison of Figs. 3.1a and 3.1b shows that while the pattern of rainfall agrees qualitatively with observations for the integrations with the excessive evaporation hydrology and low albedos over deserts and semi-arid regions (Experiment 1), the rainfall in the Northern Hemisphere deserts is about twice the observed. Comparison of Figs. 3.1b and 3.1c (Experiment 3a) shows that the increase of desert albedo and desert margin albedo from 0.14 to 0.35 results in more realistic precipitation rates over the deserts. This is seen in Table 3.3 which compares the calculated with the observed precipitation rates in the various experimental regions shown in Fig. 1.1. Comparison of Figs. 3.1b–3.1d (Experiment 3b) shows

TABLE 3.2. The latitudinal and longitudinal boundaries of the various test regions.

	Geographical region	Number of grid points	Latitude	Longitude
Marginal	Sahel	11	16°N–20°N	17.5°W–37.5°E
	Rajputana	4	24°N–32°N	67.5°E–77.5°E
	Western Great Plains	8	32°N–48°N	107.5°W–97.5°W
Humid	Central Africa	13	8°N–12°N	12.5°W–52.5°E
	Bangladesh	4	20°N–28°N	77.5°E–87.5°E
	Mississippi Valley*	7	32°N–48°N	92.5°W–82.5°W

* Except 44–48°N and 82.5–87.5°W representing the Great Lakes.

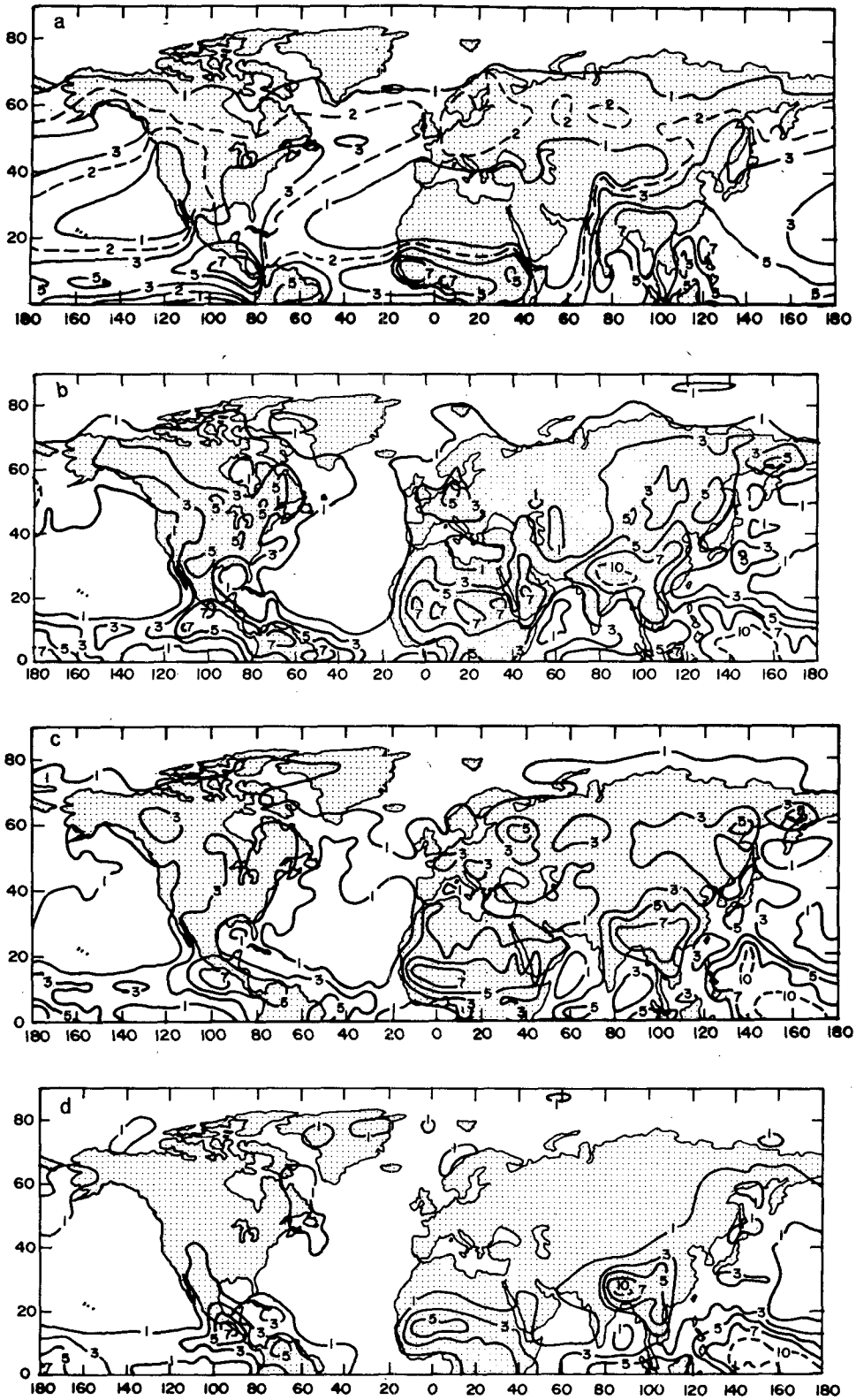

FIG. 3.1(a). Observed June–August mean rainfall (mm day^{-1}) [Möller (1951) as analyzed by Schutz and Gates (1972)] and July mean rainfall (mm day^{-1}) for (b) the excessive evaporation model with desert and desert margin albedo=0.14, Experiment 1; (c) the excessive evaporation model with desert albedo and desert margin albedo=0.35, Experiment 3a; and (d) the negligible evaporation model with desert albedo and desert margin albedo=0.35, Experiment 3b.

TABLE 3.3. Calculated and observed precipitation rates (mm day^{-1}) over desert and monsoon regions in July.

	Calculated		
	Albedo = 0.14*	Albedo = 0.35**	Observed
Desert regions			
Sahara and Arabian	4.21	2.63	0.18
Middle Eastern Desert	4.75	1.09	0.46
Central and Eastern Asiatic Desert	3.40	1.96	1.24
Great Western Desert	2.37	1.01	0.47
Monsoon regions			
Central Africa	4.16	6.27	5.07
Mississippi Valley	3.54	2.23	1.94
Bangladesh	9.31	7.64	7.94

* Experiment 1 in Table 3.1.
** Experiment 2a in Table 3.1.

that the decrease in precipitation due to the suppression of evapotranspiration is as large as the decrease due to the increase of albedo. In both high desert albedo cases the rainfall maximum in the Sahara remains some 4° latitude too far north. The remaining figures described in this section pertain to experiments with high albedos for both desert and semiarid regions (Experiments 3a and 3b).

Zonal averages of precipitation were computed for land and ocean for both the excessive and negligible evaporation hydrologies. These are shown in Fig. 3.2. Over land, the rainfall is too high in the high evaporation case and too low in the negligible evaporation case. Also, the tropical rainbelts of both models are about 4° latitude too far north (Fig. 3.2a). Over the oceans, both hydrologies give too little extratropical rainfall, and the computed maximum tropical rainfall is at the equator whereas the observed maximum is nearly 10° north of the equator (Fig. 3.2b).

The Northern Hemisphere distributions of observed and simulated evaporation rates are compared in Figs. 3.3a and 3.3b for the excessive evaporation hydrology.[3] The model evaporation rates are much larger than the observed over land and much lower over the oceans. Longitudinal averages over land are shown in

[3] What are called "observed" rates are actually inferences from the surface heat balance.

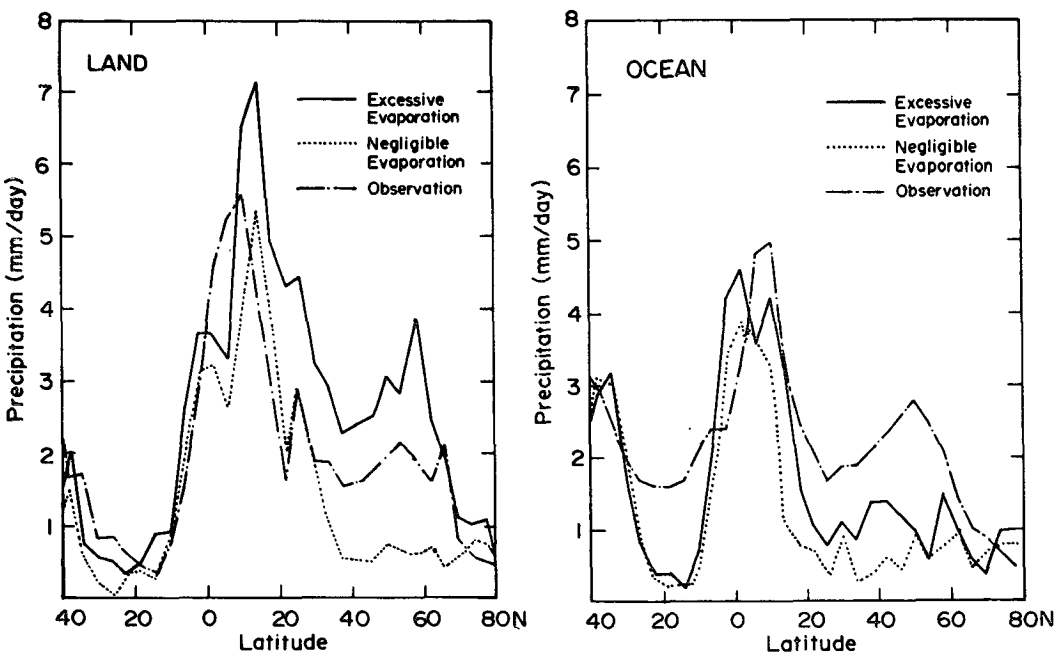

FIG. 3.2. July mean rainfall (mm day^{-1}) zonally averaged over longitude for the excessive and negligible evaporation cases with desert albedo and desert margin albedo = 0.35 and observed June, July, August mean rainfall (a) over land (b) over ocean.

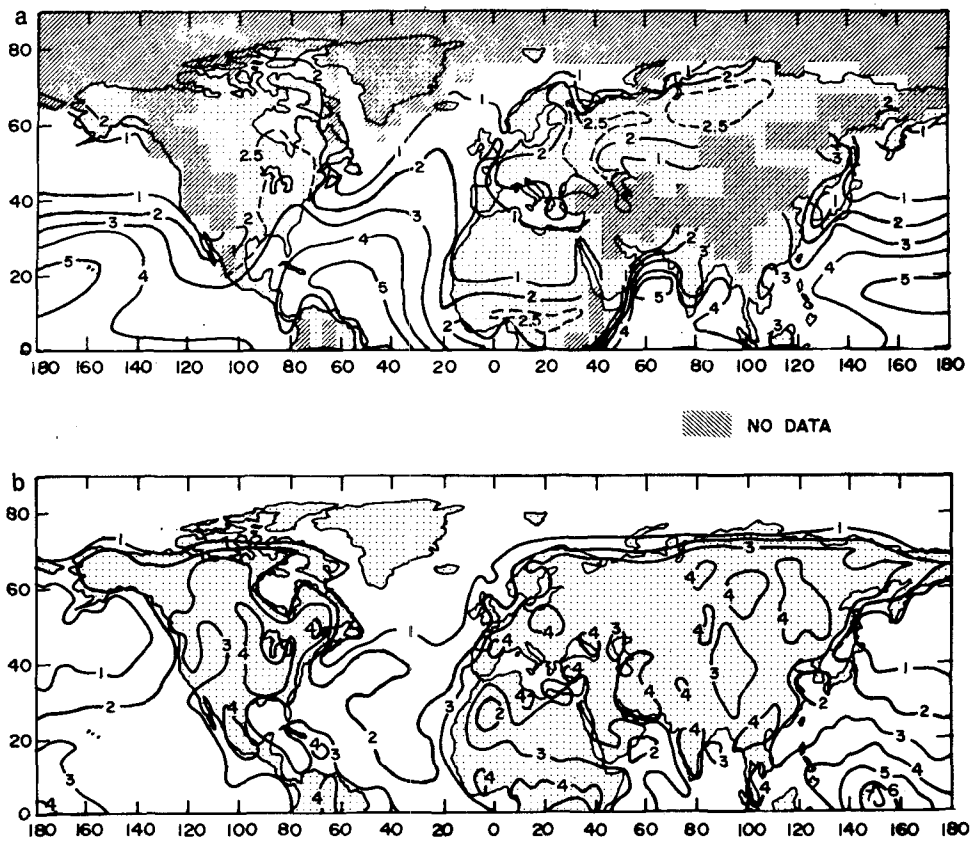

FIG. 3.3a. The observed July mean surface evaporation (mm day^{-1}) [Budyko (1963) as analyzed by Schutz and Gates (1972)]. Note: while data are not available over large regions, this is the best estimate available of global distributions of evaporation.

FIG. 3.3b. July mean surface evaporation (mm day^{-1}) in the excessive evaporation model with desert albedo and desert margin albedo=0.35, Experiment 3a.

Fig. 3.4 for both hydrologies. It may be seen that the evaporation is indeed about twice the observed for the excessive evaporation case and negligible for the low evaporation case.

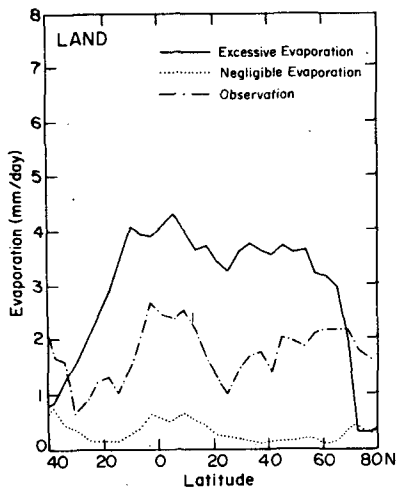

FIG. 3.4. July mean surface evaporation (mm day^{-1}) zonally averaged over land for the excessive and negligible evaporation cases with desert albedo and desert margin albedo=0.35 and observed mean surface evaporation.

b. Model Climatology for Africa

The original experiments were designed primarily to explore the effects of albedo changes on the semi-arid Sahelian zone of North Africa. As it turned out, the model climatology for July placed the mean African Intertropical Convergence Zone (ITCZ) some 4° latitude too far north, and as a consequence the zone chosen for the albedo change corresponded climatically more to the African Savanna than to the Sahel. Although the effects of albedo changes were simulated in other regions as well, the following describes only the mean July conditions over Africa for Experiments 3a and 3b of Table 3.1 and compares them with observations. The comparisons are intended to illustrate the accuracy of the model in simulating monsoonal-desert conditions. The rainfall in and near the ITCZ is associated with traveling easterly disturbances, and the extent to which the model simulates these disturbances are also described.

Figs. 3.5–3.7 show the sea level pressure, surface temperature and 950 mb relative humidities for both hydrologies as well as the observed fields. The patterns of sea level pressure and surface temperature simulated for the excessive evaporation case are seen

to be qualitatively in agreement with observations. An east-west elongated thermal low in the Sahara is clearly shown in the sea level pressure and surface temperature. In the negligible evaporation case, the low-pressure system is far too deep; the minimum sea level pressure is about 12 mb below the observed. This is because with negligible evaporation virtually all the incident solar radiation goes to heat the ground,

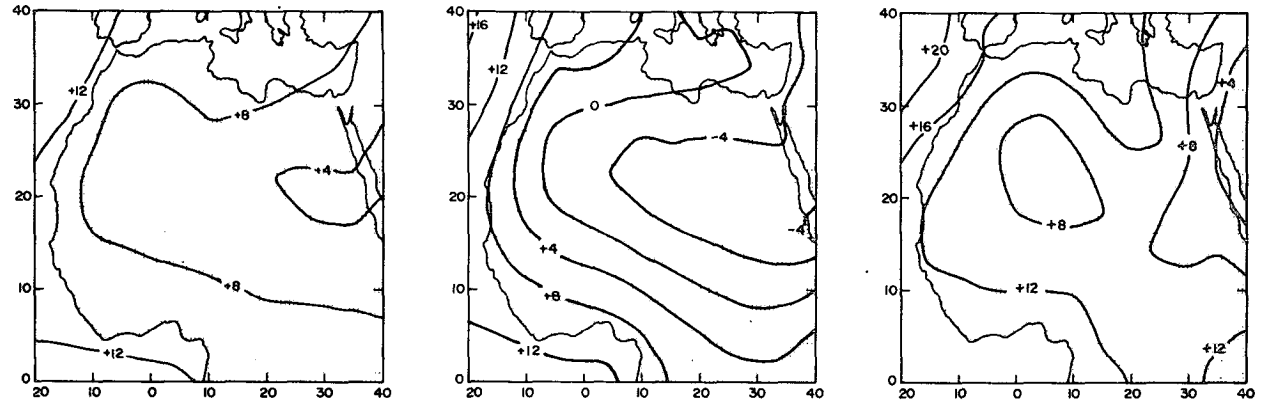

FIG. 3.5. July mean sea level pressure (mb−1000) over Africa: (a) the excessive albedo=0.35; (b) the negligible evaporation model with desert albedo and desert margin albedo=0.35; (c) observed [Crutcher and Meserve (1970) analyzed by Schutz and Gates (1972)].

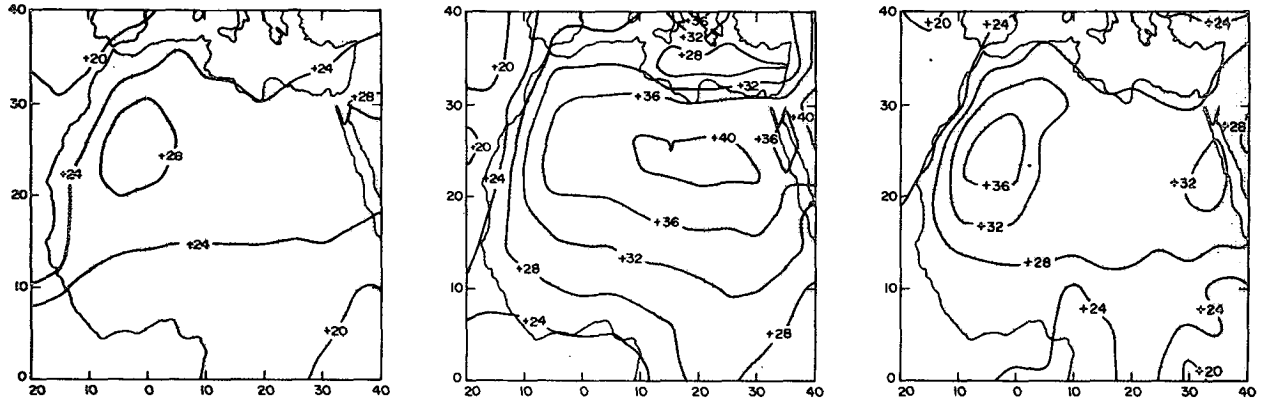

FIG. 3.6. July mean surface air temperature (°C) over Africa: (a) the excessive evaporation model with desert albedo and desert margin albedo=0.35; (b) the negligible evaporation model with desert albedo and desert margin albedo=0.35; (c) observed [Crutcher and Meserve (1970) analyzed by Schutz and Gates (1972)].

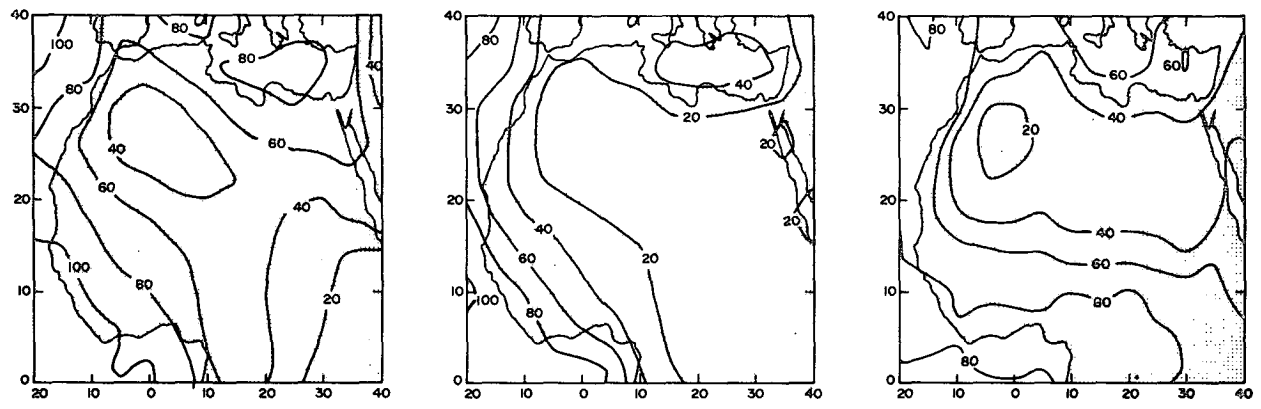

FIG. 3.7. July mean relative humidity (%) at 950 mb over Africa: (a) the excessive evaporation model with desert albedo and desert margin albedo=0.35; (b) the negligible evaporation model with desert albedo and desert margin albedo=0.35; (c) observed surface [Crutcher and Meserve (1970) analyzed by Schutz and Gates (1972)].

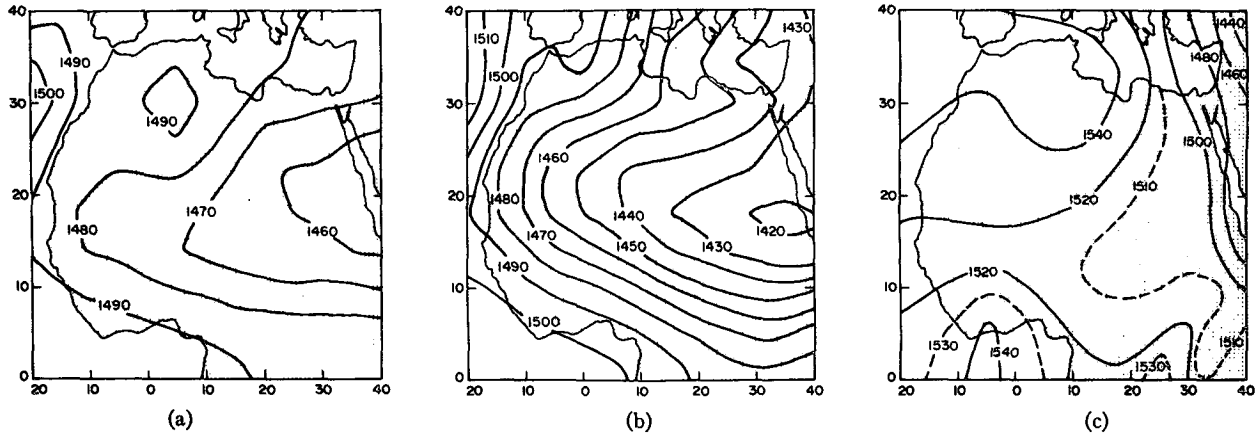

FIG. 3.8. July mean 850 mb height fields (gpm) over Africa: (a) the excessive evaporation model with desert albedo and desert margin albedo = 0.35; (b) the negligible evaporation model with desert albedo and desert margin albedo = 0.35; (c) observed (Thompson, 1965).

and the resultant high temperatures and heat fluxes—the maximum surface temperature is about 7°C higher than observed—produce an extreme heat low. In the Sahara the relative humidities are too high for excessive evaporation and about right for negligible evaporation. In both hydrologies there is an unexplained dryness at lower latitudes.

It is seen from Figs. 3.8 and 3.9 that the 850 and 700 mb height fields simulated by the excessive evaporation model hydrology are qualitatively in agreement with observation but about 50 and 80 gpm, respectively, too low. For example, the ridges over northwest Africa and the trough axis lying near the southern margin of the Sahara are all clearly marked. As at sea level, the fields are shifted somewhat northward of the climatic average for the period June–August, but the shift is not as great as that of the rainbelt from its normal position. The weakness of the 850 and 700 mb highs in northwest Africa in the excessive evaporation case, and their absence at 850 mb in the negligible evaporation case, is associated with a deficiency of horizontal divergence and sinking motion at these levels. This reduces the sinking and spreading southward of the dry desert air and allows the monsoon rainfall to penetrate too far northward.

Figs. 3.10 and 3.11 show the July mean vertical motion and rainfall respectively. The two are closely correlated. In the excessive evaporation case it is again seen that the rainfall patterns are located about 4° too far to the north. The upward motion is weaker than in the negligible evaporation case, but the rainfall is greater because the air is more humid. The cloud cover is closely correlated with rainfall, as may be seen from Tables 4.1 and 4.2 and, like evaporation and rainfall, is found to be excessive over land. Global maps of cloud cover for Experiment 1 are presented in Stone *et al.* (1977).

Near the surface the dry northeast wind and the moist southwest wind converge at the so-called Intertropical Front (ITF), which coincides with the axis of the east-west elongated thermal low, but the rainfall is not found in the vicinity of the ITF. According to Godske *et al.* (1957), this is because the dry desert air which overruns the cooler, moister maritime tropical

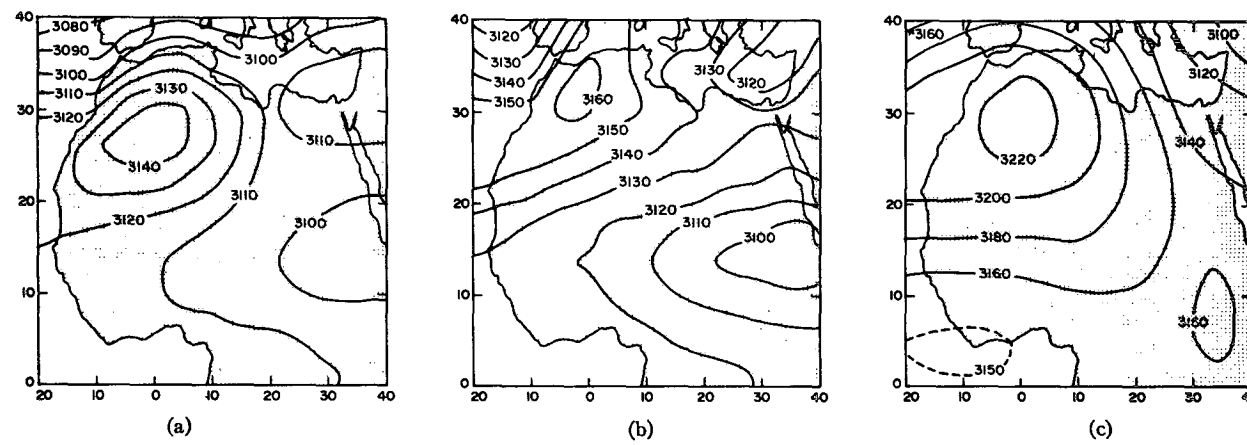

FIG. 3.9. As in Fig. 3.8 except for 700 mb height fields.

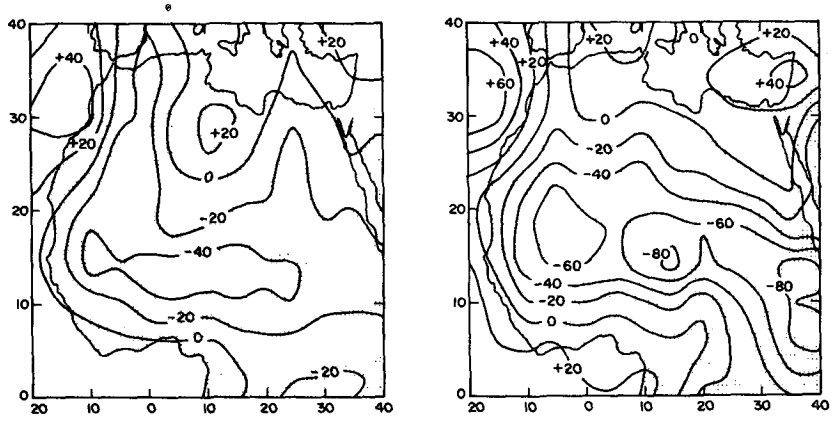

FIG. 3.10. July mean 700 mb vertical wind [$\omega = dp/dt$ (mb day^{-1})] over Africa: (a) the excessive evaporation model with desert albedo and desert margin albedo = 0.35; (b) the negligible evaporation model with desert albedo and desert margin albedo = 0.35.

air to the south of the front effectively suppresses the convection that originates in the shallow layer of moist air. Only considerably to the south of the front, where the maritime air is thick enough to support internal convection, does rainfall occur.

Dynamically, the absence of rain near the ITF was explained by Charney (1975) as due to a frictionally controlled circulation induced by the high albedo of the desert combined with strong, dry convection in its lower layers. Low-level convectional heating of the desert air and high-level radiative cooling cause the monsoon current to flow to the north of the rain zone near the ground and return upward and southward aloft in a thin wedge. Above this wedge the radiative cooling causes the desert air to sink and spread southward until it encounters the rising air in the rain zone. The dry sinking desert air above the wedge of monsoon air suppresses deep cumulus convection.

Mean meridional cross sections for the simulations of temperature, zonal wind component and vertical motion at 10°E for July are shown in Figs. 3.12–3.14. For comparison the observed cross section of zonal wind for August (Burpee, 1972) is shown in Fig. 3.15. The corresponding sections at 30°E (not presented here) indicate a considerable degree of zonal symmetry over northern Africa. It may be seen here and in Fig. 3.6 that the surface temperatures over the Sahara are too low in the high evaporation case and too high in the low evaporation case, so that the associated thermal winds to the south of the temperature maximum are too weak in the former case and too strong in the latter. The thermal winds give rise to horizontal shears which are also too weak in the former case and too strong in the latter. Hence large amounts of zonal potential and kinetic energy are available in the negligible evaporation case for con-

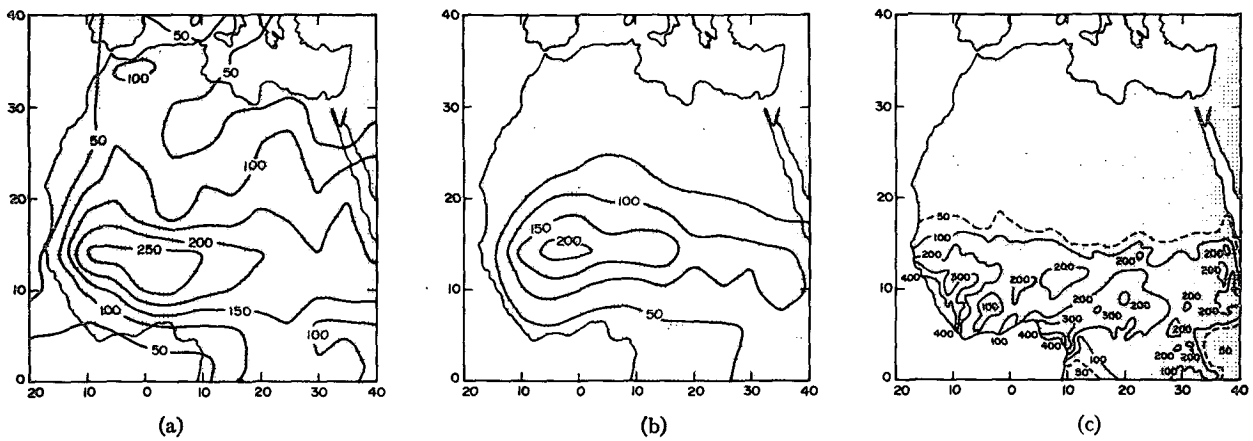

FIG. 3.11. July mean rainfall (mm month^{-1}) over Africa: (a) the excessive evaporation model with desert albedo and desert margin albedo = 0.35; (b) the negligible evaporation model with desert albedo and desert margin albedo = 0.35; (c) observed (Thompson, 1965).

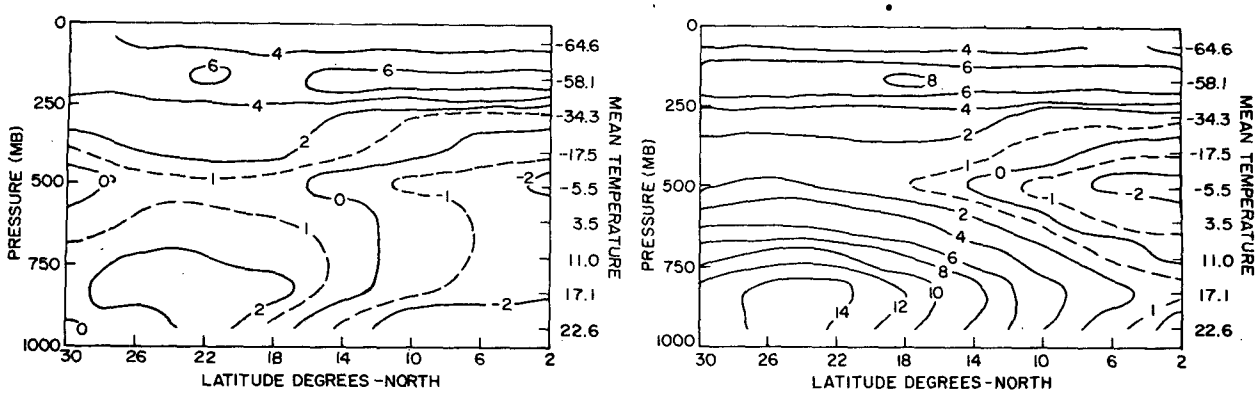

FIG. 3.12. Meridional cross section of the July mean temperature anomaly (°C) at 10°E. The anomaly is calculated as a deviation from a mean sounding which is given on the right hand ordinate. (a) The excessive evaporation model with desert albedo and desert margin albedo = 0.35, (b) the negligible evaporation model with desert albedo and desert margin albedo = 0.35.

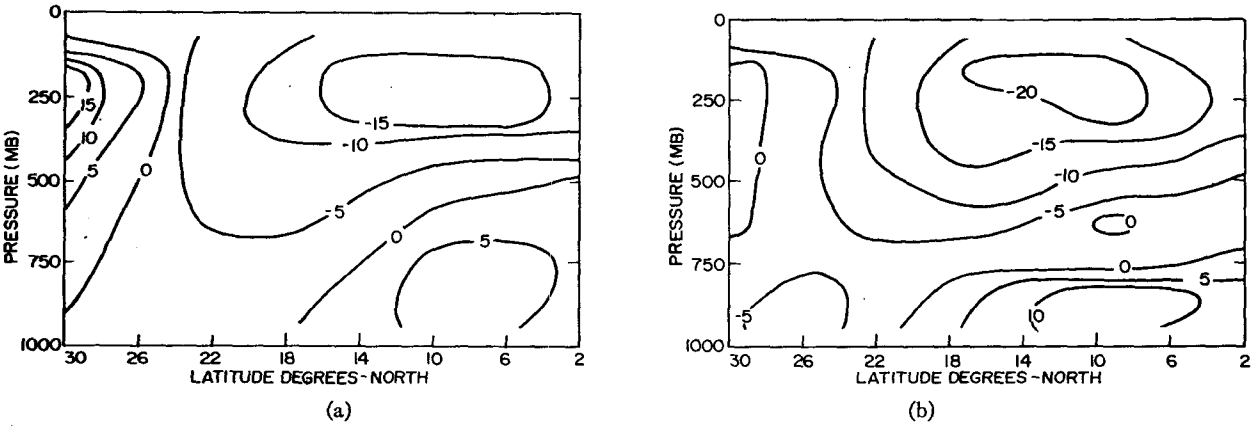

FIG. 3.13. Meridional cross sections of the July mean zonal wind (U, m s^{-1}) at 10°E: (a) the excessive evaporation model with desert albedo and desert margin albedo = 0.35; (b) the negligible evaporation model with desert albedo and desert margin albedo = 0.35.

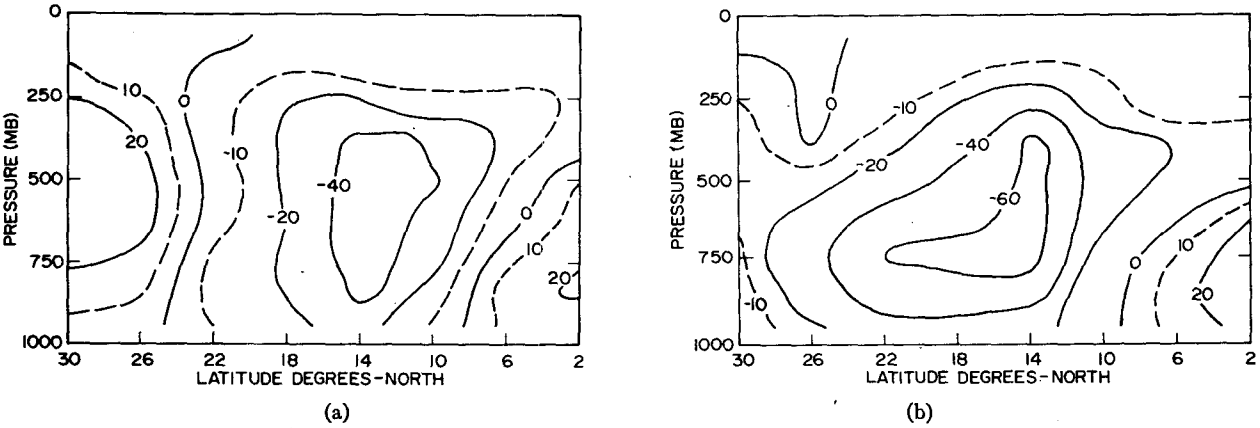

FIG. 3.14. Meridional cross sections of the July mean vertical wind (ω, mb day^{-1}) at 10°E: (a) the excessive evaporation model with desert albedo and desert margin albedo = 0.35; (b) the negligible evaporation model with desert albedo and desert margin albedo = 0.35.

version to disturbance energy, whereas only small amounts of these quantities are available in the high evaporation case. In the former, baroclinic and barotropic instability exist separately, and disturbances form to convert both forms of energy. In the latter, the zonal flow is only weakly unstable baroclinically and not at all unstable barotropically (no maximum of the vertical component of the absolute vorticity).

The result is that the disturbances in the former (negligible evaporation) case are stronger and more regular than those in the latter. This may be seen in Figs. 3.16 and 3.17 showing daily charts of 850 mb heights and the associated rainfall patterns for a 12-day period during the month of July. The shaded areas indicate rainfall rates in excess of 5 mm day^{-1} during the 25 h period centered approximately at 1200 GMT. In the negligible evaporation case, the mean wavelength is about 25° of longitude, the phase velocity 6–7° longitude day^{-1}, and the maximum rainfall occurs to the west and south of the low center. These properties are in approximate agreement with the observations reported by Carlson (1969). However, when the disturbances approach the west coast of Africa they tend to stagnate and show little tendency to propagate over the Atlantic. This behavior gives a maximum of precipitation inland rather than at the coast (Fig. 3.11).

Disturbances also form in the excessive evaporation model, but there is little evidence of regular motion, and the precipitation, while more copious, is more randomly distributed. It seems clear that a more realistic treatment of hydrology would have led to improved dynamics. The evaporation would have been more moderate, and the temperatures over the desert lower than in the negligible evaporation case but, one expects, high enough to produce the required instabilities and rainfall distributions.

4. Numerical simulations of the effects of regional albedo changes

To test the effects of changes in albedo on July rainfall, the following experiments were performed.

a. Desert margin experiments

Control integrations for the month of July were carried out with albedos of 0.35 over the idealized desert areas and 0.14 over all other land areas except in polar regions. These are Experiments 2a and 2b of Table 3.1. In Experiments 3a and 3b the albedos of the idealized Sahel, Rajputana and western Great Plains regions (shown as cross-hatched areas in Fig. 1.1, with latitude and longitude intervals given in Table 3.2) were raised to 0.35 and the integration was repeated for both the excessive and negligible evaporation hydrologies. In order to obtain a representative July average, the integrations were begun on 18 June and continued to the end of July. This was done because it required ~1 day for dynamical adjustment and ~10 days for cloud and water vapor adjustment following a change in albedo or ground wetness. If the ground wetness had not been kept fixed, a much longer period would have been required for adjustment between the moisture in the ground and the moisture in the air.

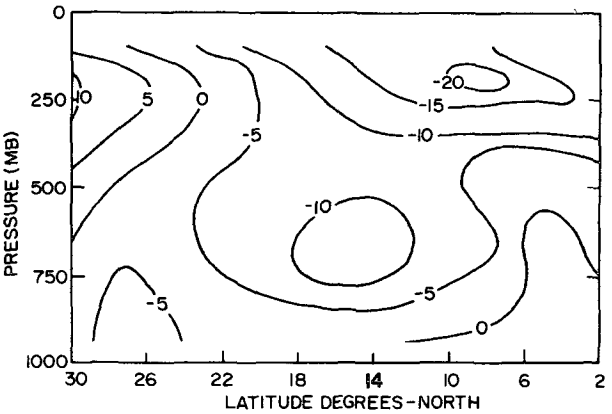

FIG. 3.15. Observed meridional cross sections of August mean zonal wind (U, m s^{-1}) at 5°E (Burpee, 1972).

b. Humid region experiment

For Experiment 4, regions similar in size and shape to the semi-arid regions of Experiment 2 were chosen in adjacent humid areas in central Africa, the Mississippi Valley and in Bangladesh. These are shown as the heavy dotted areas of Fig. 1.1. The integration was carried out for the excessive evaporation case only.

An analysis of the six experiments is contained in Tables 4.1–4.5. The albedo increase in the three semi-arid regions caused an appreciable reduction of precipitation in all three regions with the excessive evaporation hydrology, but only in the Sahel and perhaps the western Great Plains with the negligible evaporation hydrology. Since evaporation is comparable with precipitation in both the Rajputana and western Great Plains regions, it is not surprising that the reduction of the evaporation to negligible proportions greatly affected the rainfall in these regions, especially in the western Great Plains where evaporation actually exceeded precipitation.

Figs. 4.1–4.3 show the change in rainfall due to an increase of albedo in the semi-arid regions for the high evaporation case. The geographical distribution of the changes makes it clear that a reduction in precipitation everywhere accompanied an increase of albedo. The charts also show that *increases* of rainfall took place to the southwest of the Sahel, to the south and southeast of the Rajputana region, and to the southeast of the western Great Plains. These increases represent shifts of the associated monsoon rain areas induced by the albedo changes in the semi-arid regions.

To establish the reliability of the results of our experiments it must be shown that the albedo-induced changes are greater than changes resulting from random fluctuations. The degree of the noisiness in the test areas may be inferred from Figs. 4.4 and 4.5 which show the weekly averages of precipitation for Experiments 2a, 2b, 3a and 3b. In the excessive evaporation case the reduction in precipitation is seen

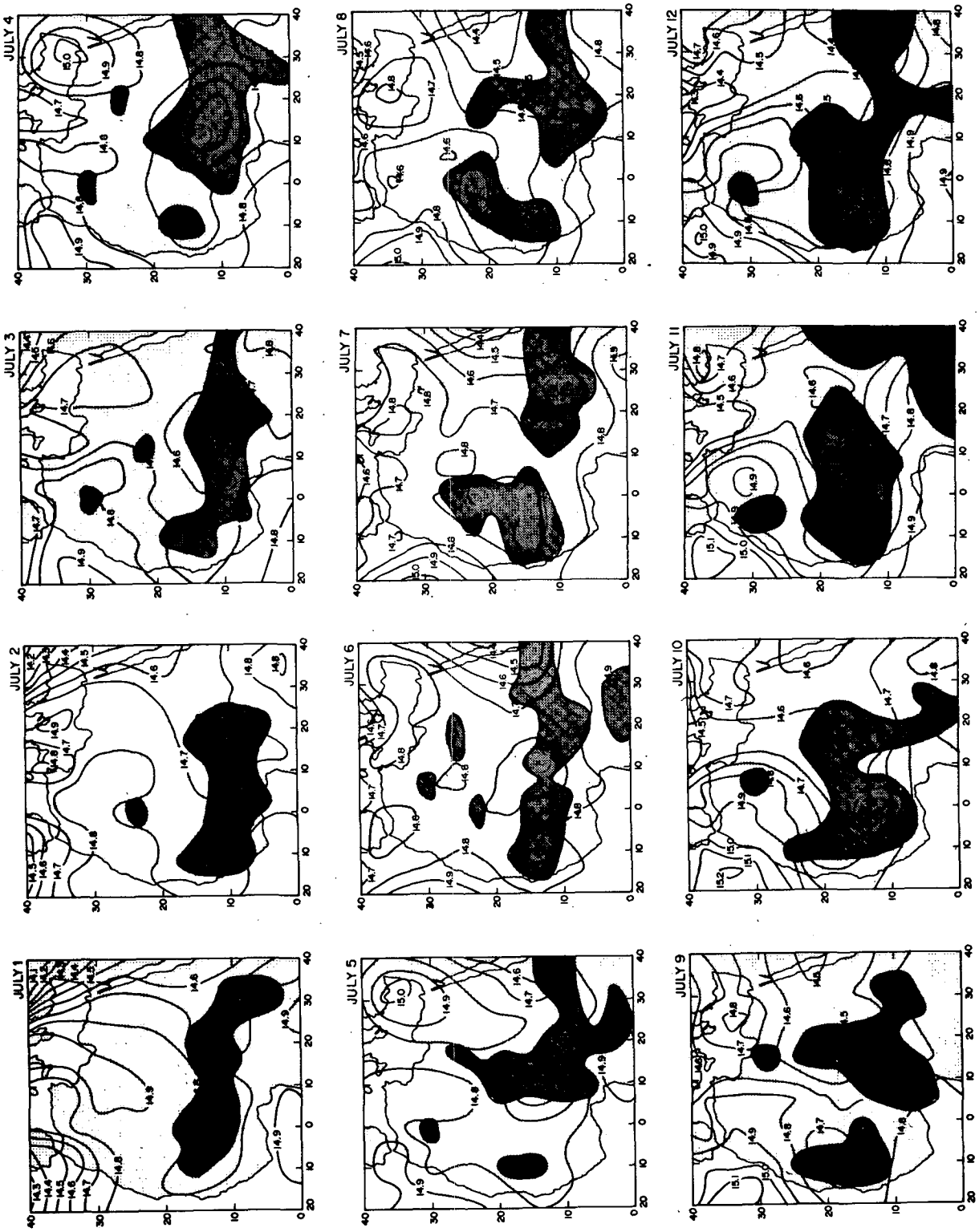

FIG. 3.16. Synoptic charts from the excessive evaporation model with desert albedo and desert margin albedo = 0.35 for 1–12 July. Shaded areas show rainfall rates >5 mm day^{-1} for the half-hour before 1200 GMT. Contours show 850 mb heights in units of 100 gpm.

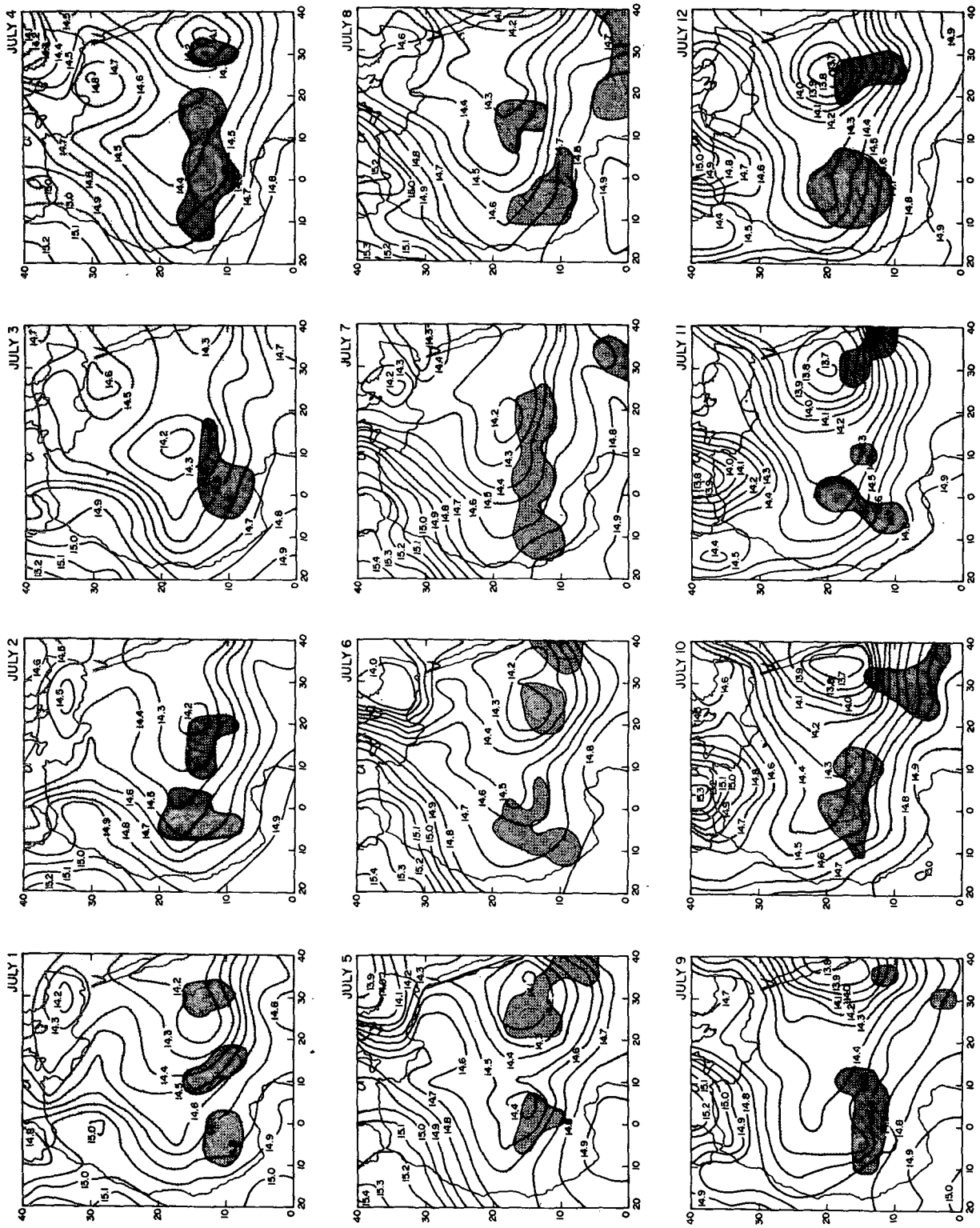

FIG. 3.17. As in 3.16 except for the negligible evaporation model with desert albedo and desert margin albedo = 0.35.

TABLE 4.1. Precipitation and evaporation for the excessive and negligible evaporation models. The number to the left of the slash is precipitation, to the right, evaporation. Units: mm day^{-1}.

		Excessive evaporation		Negligible evaporation	
		Albedo		Albedo	
	Observed	14%	35%	14%	35%
Sahel	1.2/0.9	7.4/3.7	4.0/2.8	4.0/0.14	2.7/0.34
Rajputana	2.7/1.9	4.9/4.1	2.3/3.6	2.1/0.10	2.4/0.26
Western Great Plains	1.9/2.3	3.7/4.2	2.2/3.2	0.8/0.004	0.4/0.10
Central Africa	5.1/2.2	5.0/4.3	1.9/3.6	3.1/0.18	
Bangladesh	7.9/3.1	8.0/3.9	8.0/3.7	4.6/0.38	
Mississippi Valley	2.3/2.8	4.4/5.1	3.3/3.5	1.2/0.08	

to persist from week to week for each region, except in the western Great Plains where no reduction took place in the second week. In the negligible evaporation case, the results are less definite. A significant net reduction seems to have taken place in the Sahel and perhaps the western Great Plains, but the change in the Rajputana region is small compared to the weekly variation in rainfall.

In the humid area experiment, Table 4.1 shows an appreciable reduction of rainfall in central Africa, a lesser reduction in the Mississippi Valley and no reduction in Bangladesh. It may be important that the evaporation is comparable to the rainfall in the first two regions but is only half as large in the third region, where, additionally, advective effects are stronger; condensational heating in the foothills of the Himalayas and sensible heating in the Himalayas and Tibetan plateau draw a swift moist air current over the Bangladesh area.

5. Discussion

The mechanism by which an increase of albedo caused cooling of the air and a decrease of precipitation in the presence of vegetation and ground moisture was found to be more complicated than that postulated by Charney (1975) for a desert with no evaporation.

TABLE 4.2. Total cloud cover (left of slash) and penetrating convective cloud cover (right of slash).

	Excessive evaporation		Negligible evaporation	
	Albedo		Albedo	
	14%	35%	14%	35%
Sahel	69.7/40.5	46.0/25.5	40.1/10.6	34.8/10.4
Rajputana	77.2/31.3	56.9/18.3	43.2/12.1	41.8/11.8
Western Great Plains	66.6/26.0	51.6/19.3	21.4/4.3	19.6/3.2
Central Africa	71.6/19.8	59.3/11.9	55.6/9.6	
Bangladesh	85.1/37.8	78.5/29.8	65.5/16.3	
Mississippi Valley	57.1/21.0	55.6/25.1	24.6/5.4	

TABLE 4.3. Absorbed solar radiation (left of slash) and radiation balance at the ground (right of slash). Units: ly day^{-1}.

	Excessive evaporation		Negligible evaporation	
	Albedo		Albedo	
	14%	35%	14%	35%
Sahel	355/233	372/196	544/253	447/154
Rajputana	378/278	397/239	565/283	459/189
Western Great Plains	391/260	388/222	636/272	515/177
Central Africa	358/240	359/215	479/242	
Bangladesh	312/234	294/201	434/232	
Mississippi Valley	436/294	357/217	612/271	

Although the increase of albedo reduced the absorption of solar radiation by the ground, it also reduced the transfer of sensible plus latent heat to the atmosphere. This caused a reduction in cloud and precipitation, and therefore a decrease in the planetary albedo. Indeed, in most cases the reduction in cloud amount was so great that the decrease of cloud albedo overrode the increase of ground albedo and caused a net increase in the absorption of solar radiation at the ground. However, in proportion to the reduction in cloudiness, there was an even greater increase in the net loss of longwave radiation from the ground, since the downward longwave radiation from a cloud (acting as a blackbody at base temperature) is much greater than that from a cloudless atmosphere. *The result was that the net absorption of solar plus longwave radiation by the ground was decreased.* Thus Table 4.2 shows that in the excessive evaporation case the increase of albedo from 0.14 to 0.35 in the semi-arid regions caused a decrease of cloud cover, whereas Table 4.3 shows that while the ground absorption of solar radiation was thereby increased or held nearly constant, the absorption of solar plus longwave radiation was decreased an average of 36 cal cm^{-2} day^{-1}. Since the heat capacity of the ground was negligible, this meant that there was an almost equal decrease in the transfer of sensible plus latent heat to the

TABLE 4.4. Surface air temperature (C°).

		Excessive evaporation		Negligible evaporation	
		Albedo		Albedo	
	Observed	14%	35%	14%	35%
Sahel	31.4	26.0	25.7	39.2	36.1
Rajputana	32.1	24.9	24.1	35.1	34.2
Western Great Plains	24.2	21.1	19.0	37.5	31.4
Central Africa	25.6	22.2	21.6	32.2	
Bangladesh	27.6	24.2	23.6	31.8	
Mississippi Valley	24.2	22.1	22.6	40.0	

TABLE 4.5. Rainfall for the various regions (mm day^{-1}) from four model integrations with 14% albedo over all land surfaces except in polar regions. The four integrations differ because of randomly distributed perturbations inserted in the initial conditions, with rms values of 3 m s^{-1} in wind and 1°C in temperature.

	Control	Predictability experiments 1	2	3	Standard deviation
Sahel	6.90	6.39	7.14	6.27	0.413
Rajputana	6.66	7.39	7.57	7.35	0.486
Western Great Plains	3.39	4.18	3.76	3.67	0.327
Central Africa	4.20	3.84	3.96	3.74	0.198
Bangladesh	10.00	10.72	10.50	9.76	0.442
Mississippi Valley	4.18	3.77	3.87	3.97	0.175

atmosphere and therefore a decrease in cloud and precipitation.

The negligible evaporation case stands in sharp contrast. Here the effect of an albedo change is more like that of a desert. The cloudiness changes are small, and the increase of albedo causes a large decrease of heating of the ground by solar radiation alone as well as by solar plus longwave radiation.

What matters is the decreased transfer of sensible plus latent heat to the atmosphere, i.e., the transfer of moist static energy, $c_pT+Lq+gz$ (c_p=specific heat at constant temperature, T=temperature, L=specific latent heat of evaporation, q=specific humidity, g=acceleration of gravity, z=height), and if the time

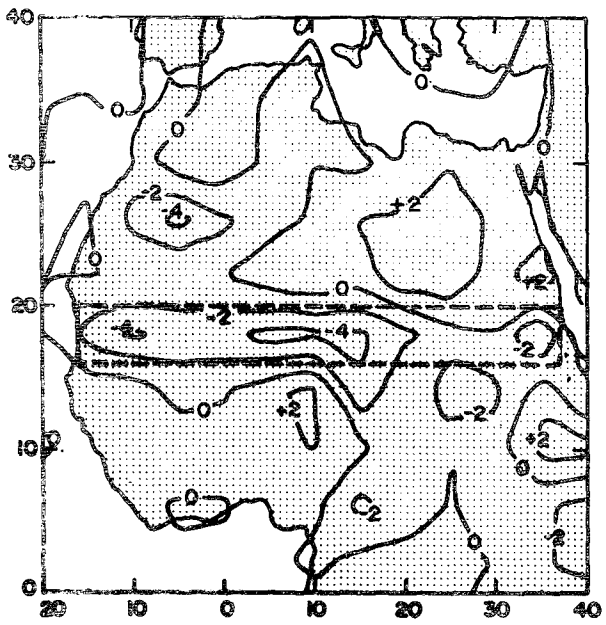

FIG. 4.1. African rainfall differences (mm day^{-1}) for July due to a change of albedo from 0.14 to 0.35 in the desert margin areas for the excessive evaporation case. The area enclosed with dashes is the area where the albedo change took place.

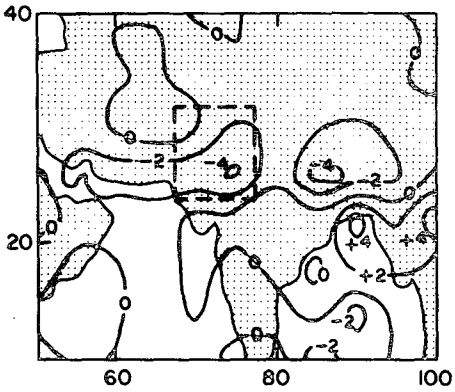

FIG. 4.2. As in Fig. 4.1 except for Asia.

scale for advecting this quantity away is less than the time scale for its accumulation, decreased cumulus convection and precipitation will occur (in the rainy season). This is what was observed in most of the experiments. The increase of albedo and the consequent reduction of the transfer of sensible and latent heat to the air led to a cooling which either increased low-level horizontal divergence and sinking or else reduced low-level horizontal convergence and rising. The perturbation in vertical motion dried the air and reduced the rainfall still further, i.e., the dynamical and thermodynamical effects supported one another.

The dynamical processes by which the cooling causes a decrease in vertical motion depend very much on the scale of the area over which the albedo changes occur. The mechanism postulated by Charney (1975) in his Symons Memorial Lecture was a frictionally controlled, quasi-geostrophic circulation driven by the temperature contrast, level for level, between the nearly dry adiabatically decreasing (at low levels) radiative equilibrium temperature over the desert and the moist adiabatically decreasing temperature in the ITCZ at the southern margin of the desert. Using the semi-transparent approximation for the vertical transfer of radiation, Charney showed that sinking

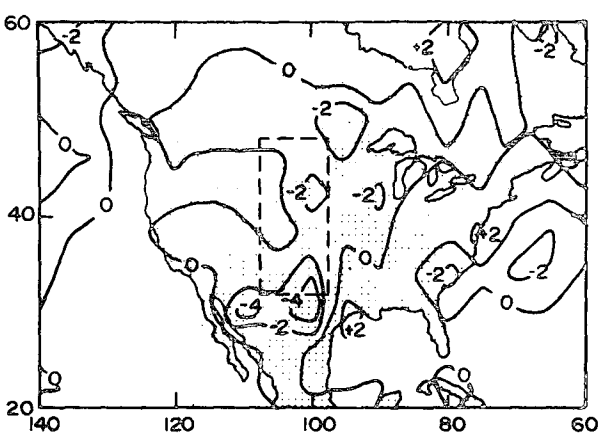

FIG. 4.3. As in Fig. 4.1 except for North America.

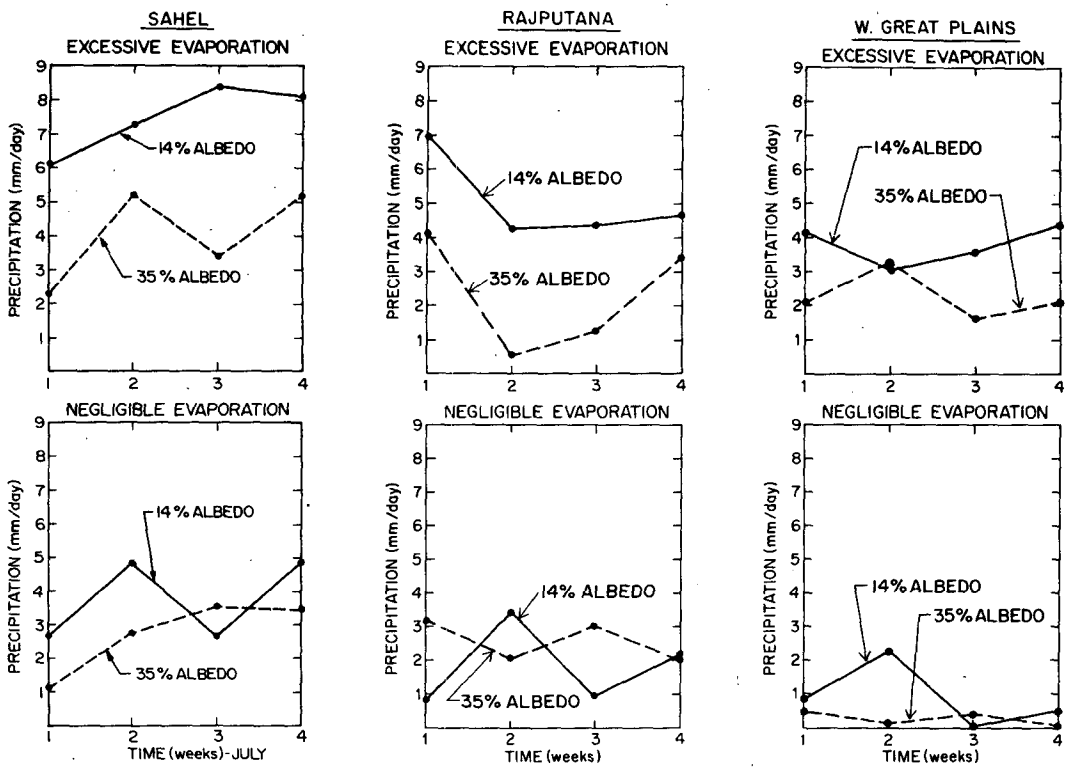

FIG. 4.4. Weekly average rainfall rates (mm day^{-1}) for July over selected areas for Experiments 2a and 2b (14% albedo in the regions) and 3a and 3b (35% albedo in the regions).

motion occurs at levels where the desert equilibrium temperatures are lower than the ITCZ temperatures, and rising motion occurs where they are higher. This accounts for the seemingly paradoxical result that the air aloft sinks over the desert despite the fact that its surface is hotter than surrounding surfaces. The explanation given by Charney is that there is indeed a shallow layer of rising air near the ground which underlies the sinking air. The existence of this shallow layer, which underlies the Intertropical Front and mixes with the dry descending air aloft, would seem to account for the shift of the rain area to the south of the monsoon trough axis (see Section 3).

Ripley (1976) has pointed out that when a region is denuded of vegetation and the albedo thereby increased, the evapotranspiration may be so decreased that the reduction in the latent heat transfer may exceed the reduction of adsorbed solar radiation and cause the temperature of the ground to rise. That this was indeed the case may be seen from Table 4.4. When the evaporation was high and the albedo 0.14, the ground temperatures averaged 24°C; when the

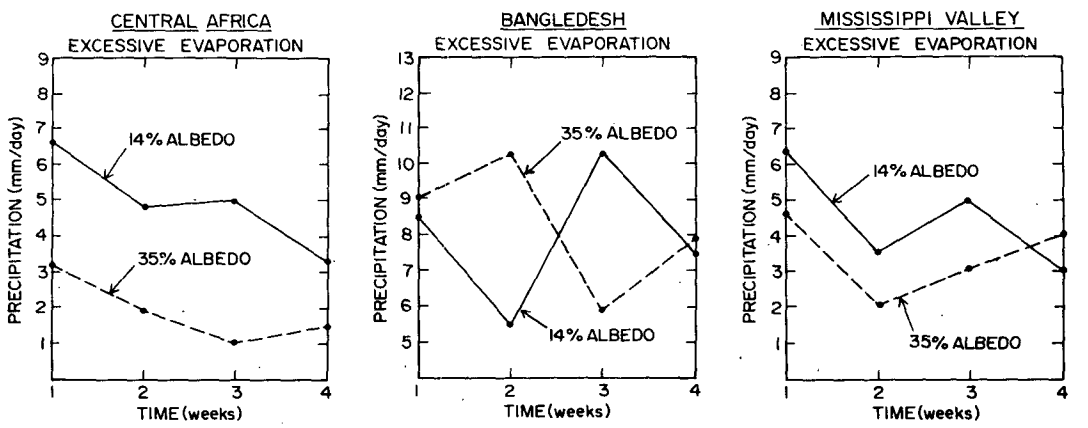

FIG. 4.5. As in Fig. 4.4 except for Experiments 2a (14% albedo in the regions) and 4 (35% albedo in the regions).

evaporation was negligible and the albedo 0.35, the ground temperatures averaged 34°C. But contrary to Ripley's contention, the rainfall decreased with the increase of surface temperature.

One cannot establish a simple connection between the temperature change at the ground and the change in rainfall. Thus Tables 4.1 and 4.4 show that no such correlation exists for the high-evaporation mode, and although there was a correlation for the negligible evaporation model, it was negative. Ripley is correct in his emphasis on the importance of the decrease in evapotranspiration, as well as increase in albedo, when the plant cover is reduced, but both act to *decrease* the rainfall. Thus Table 4.1 shows that the reduction of evapotranspiration (over all the continents) from excessive to negligible decreased the rainfall in the semi-arid regions with low albedo as much as raising the albedos from 0.14 to 0.35. In future simulations of the meteorological consequences of modifying plant cover, it will be important to take into account changes in evapotranspiration as well as changes in albedo. It will also be necessary to consider the changes in albedo caused by the wetting of the ground. All of the above effects increase the biogeophysical feedback effect originally postulated by Charney.

We repeat (Charney *et al.*, 1975) that our results cannot be explained as being due to a thermally forced, gravity-wave perturbation of a mean flow, as suggested by Otterman (1974). Such an effect could conceivably occur for albedo changes of small dimension and in the presence of strong advection. But if, as Ripley suggests, an increase in plant cover causes an increase in evapotranspiration as well as a decrease in albedo, there may be no increase in the surface temperature, and the direct thermal forcing postulated by Otterman may not exist. It is possible that the north side of the Egyptian-Israeli armistice line with its sparse vegetation but appreciable debris may be an exception (Otterman *et al.*, 1976). If, as Otterman maintains, a large contrast in albedo exists across the line without an appreciable change in evapotranspiration, the western Negev may indeed be modeled as by an equivalent thermal mountain some 40 km across.

The smallest linear dimension of a test area in our numerical experiments was one grid interval, about 400 km. It might be expected that the truncation error will have been large for this case, but it is difficult to see how it could alter the qualitative character of our results. Nevertheless, in the Appendix we present a quantitative estimate of the error in a simple case. The analysis indicates that the error is in fact quite small.

What is the least dimension of the area for which albedo and ground moisture changes can be expected to influence convective rainfall? A plausible rule of thumb would seem to be that observable effects can be expected when the characteristic time for a change in the surface flux of moist static energy, $c_pT+Lq+gz$, to penetrate to cloud base is smaller than the time required for new properties to be advected into the region. If we take 2–4 h for the former time and, say, 20 km h^{-1} for the advection velocity, we arrive at a minimum dimension of 40–80 km. It should be possible to check this estimate by means of surface observations of albedo and soil moisture combined with satellite observations of convective cloud. Some efforts of this kind are now under way. Obviously, there will be no effect if the air is not sufficiently moist already. Hence the observations should be made in the rainy season.

Leith (1973) has cautioned that one must analyze the statistical fluctuations of the model to determine the significance of changes in the mean properties of the atmosphere brought about by changes in boundary conditions. He suggested a method for computing the signal-to-noise ratio which involves comparing mean changes with standard deviations. Unfortunately, a six-month integration is needed to calculate a standard deviation to an accuracy of 25%. For this reason we were unable to use his method to evaluate the significance of our results. Nevertheless, a partial assessment of significance is afforded by a series of predictability experiments which were carried out with an earlier version of the GISS model, the one in which all land albedos were 0.14 except in polar regions (Experiment 1 in Table 3.1). A control integration was performed beginning on 18 June and extending through July, after which three more integrations were performed for the same period with random perturbations in the initial temperature and wind fields having rms values of 1°C and 3 m s^{-1}, respectively. In each case individual synoptic systems became uncorrelated by 1 July. It may be seen from Table 4.5, which shows the variations in the mean precipitation for July, that in almost all the cases the standard deviations from the control run were much smaller than the changes observed when the albedos were changed (Table 4.1).

6. Conclusions

We have shown by numerical simulation with the GISS general circulation model that appreciable changes in albedo and evaporation rate significantly affect the simulated convective cloud and precipitation on the borders of and within certain monsoonal regions of large scale ($\geq$400 km in their smallest dimension) during the summer rainy season. The changes were pronounced in the semi-arid zones adjoining the Sahara, the deserts of central Asia and the Great Western Desert of North America; they were also pronounced in central Africa and, to a lesser extent, in the Mississippi Valley.

There are two difficulties in applying our results to real situations. First, the changes in albedo were necessarily hypothetical in the absence of reliable measurements of actual albedos and albedo changes. Second, although the numerical model compares favorably with others of like complexity, it was found to be too inaccurate in its simulation of the actual climates in some of the test areas to justify more than purely qualitative conclusions concerning real situations. For example, the simulated zonally averaged rainfall maximum over Africa for July was some 4° latitude too far north—at 14°N rather than 10°N—and the Sahel region, which for the purposes of the tests was centered at 18°N, was incorrectly placed relative to the model climatology. This may be seen from Table 4.1: far too much rainfall occurs in the Sahel for both high and low albedos and for the high and low evaporation hydrologies. In relation to the model climatology it would have been better if the Sahel had been placed at 22°N. However, since the observed reduction in rainfall extended south of 14°N (Tanaka *et al.*, 1975), it may be held that the albedo change at 18°N really simulates the changes that took place at 14°N, i.e., in the Savanna region of Africa rather than the Sahel. Judging from the rainfall amounts, the remaining areas do not seem so badly placed. The fact that the model evaporation was in every case too great might well account for the major observed discrepancies in rainfall.

An obvious defect in the model is its hydrology, and efforts are being made to improve it. The simulation of cumulus convection also leaves much to be desired. However, although improvements in climate simulation can be expected to follow improvements in our understanding of the physics of the atmosphere and its mathematical treatment, considerable defects in the climate simulations can be expected to remain for some time to come. How then is one to establish the accuracy of a simulation of a regional climatic anomaly? How can one pass from the present "impact" or "sensitivity" studies to useful predictions? Let us assume that accurate measurements of atmospheric fields and boundary conditions will eventually be made, most likely with the aid of satellites. One method may be to use the general circulation models to predict only perturbations from *actual* motions which are due to observed or predicted perturbations in the boundary conditions. The latter will presumably have longer time constants than the motions themselves, and will therefore permit longer range predictions of the anomalies, provided that the signal-to-noise ratio is sufficiently high. The method would have the advantage that the changes in boundary conditions would be correctly placed with respect to the actual climate, and the results therefore directly comparable with observation.

As better general circulation models are developed, the experiments described in this article should be repeated, for it has already been remarked that the accuracy of the models for the simulation of the actual climate leaves much to be desired. Moreover, a larger ensemble of predictions will be necessary to establish the statistical significance of the results more securely. But the only way that biogeophysical feedback hypotheses of the kind offered here can finally be confirmed or disproved is by study of actual observations. If droughts over large regions are self-sustaining, then satellite monitoring of the albedo, the plant cover and the hydrology in drought-prone regions, together with other relevant boundary conditions such as sea-surface temperatures in neighboring tropical seas, must be combined with numerical simulation to enable one eventually to understand and possibly predict drought—probabilistically.

Acknowledgments. We would like to thank the director and staff of the Goddard Institute for Space Studies for their help in bringing this work to completion. Dr. Milton Halem was especially helpful, and we are also grateful to Messrs. Ming Hong, John Weiss and Gregory Baran for writing the programs which were used for obtaining and displaying our results. We would also like to thank Drs. Yale Mintz and Jagadish Shukla for a careful reading of the manuscript.

APPENDIX

Estimate of Truncation Error

To estimate the truncation error incurred when the linear dimension of a test area is a single-grid interval, we disregard evaporation and consider the thermal perturbation induced in the uniform flow of a homogeneous atmosphere by an albedo change on a strip of width a. The perturbation is not a gravity wave, but the analysis of Stern (1954) remains valid and we may replace the thermal effect by the mechanical effect of an equivalent mountain ridge of width a, especially as we seek only an estimate of the horizontal truncation error.

Let the mean height of the layer be H, the perturbation height h, the height of the ridge d and the downstream coordinate x, measured from the center of the ridge in units of the Rossby radius of deformation $(gH)^{\frac{1}{2}}/f$, where f is the Coriolis parameter. To simulate a continuously stratified atmosphere, we set $(gH)^{\frac{1}{2}}=NH$, where H is equal to the density scale height ($\sim$7 km) and N is the Brunt-Väisälä frequency ($\sim 10^{-2}$ s^{-1}), giving $(gH)^{\frac{1}{2}}/f \approx 1600$ km at 18°. If the speed of the flow is small with respect to fa ($\sim$20 m s^{-1}), the flow will be quasi-geostrophic and the motion determined from conservation of potential vorticity:

$$\frac{d^2h}{dx^2}-h=\begin{cases}-d, & |x|\leqslant a/2\\ 0, & |x|>a/2\end{cases}$$

or in finite-difference form

$$(h_{n+1}-2h_n+h_{n-1})/a^2-h_n=\begin{cases}-d, & n=0\\ 0, & n=1, 2, \ldots\end{cases}$$

$$h_n\equiv h(an), \quad h_n=h_{n-1}.$$

The solution of the former equation with the jump conditions $[h]=[dh/dx]=0$ and the condition $h=0$ at $|x|=\infty$ is

$$h=\begin{cases}d(1-e^{-a/2}\cosh x), & |x|\leqslant a/2\\ d\sinh(a/2)e^{-|x|}, & |x|>a/2\end{cases}$$

and the solution of the latter is

$$h=\begin{cases}\dfrac{da^2B}{(2+a^2)B-2e^{-\beta}}, & n=0\\ \dfrac{da^2e^{-\beta n}}{(2+a^2)B-2e^{-\beta}}, & n=1, 2, \ldots\end{cases}$$

where $\beta=\cosh^{-1}(1+a^2/2)$ and $B=(2+a^2)e^{-\beta}-e^{-2\beta}$. In the present case $a=400/1600=1/4$. For this case, $\beta\approx a$, $B\approx 1$, and the continuous formula for h is approximated by

$$h=\begin{cases}(a/2)d, & |x|\leqslant a/2\\ (a/2)de^{-|x|}, & |x|>a/2\end{cases}$$

while the finite-difference formula gives

$$h=\begin{cases}(a/2)d & n=0\\ (a/2)de^{-an}, & n=1, 2, \ldots\end{cases}$$

It is seen that the two formulas give identical values at the grid points $x=an$. Hence we may expect the results of the numerical simulation to be at least qualitatively correct.

REFERENCES

Arakawa, A., A. Katayama and Y. Mintz, 1969: Numerical simulation of the general circulation of the atmosphere. *Proc. WMO/IUGG Symp. Numerical Weather Prediction*, Tokyo, Japan Meteor. Agency, IV, 7, 8–12.

Bryson, R. A., and D. A. Baerreis, 1967: Possibilities of major climatic modification and their implications: Northwest India, a case for study. *Bull. Amer. Meteor. Soc.*, **48**, 136–142.

Buckman, O., and N. C. Brady, 1969: *The Nature and Properties of Soils*. Macmillan, 653 pp.

Budyko, M. I., 1963: *Atlas of the Heat Balance of the Earth*. Gidrometeorizdat, Moscow, 69 pp.

Burpee, R. W., 1972: The origin and structure of easterly waves in the lower troposphere of North Africa. *J. Atmos. Sci.*, **29**, 77–90.

Carlson, T. N., 1969: Some remarks on African disturbances and their progress over the tropical Atlantic. *Mon. Wea. Rev.*, **97**, 716–726.

Charney, J. G., 1975: Dynamics of deserts and drought in the Sahel. *Quart. J. Roy. Meteor. Soc.*, **101**, 193–202.

——, P. H. Stone and W. J. Quirk, 1975: Drought in the Sahara: A biogeophysical feedback mechanism. *Science*, **187**, 434–435.

——, —— and ——, 1976: Drought in the Sahara: Insufficient biogeophysical feedback? Reply. *Science*, **191**, 100–102.

Crutcher, H. L., and J. M. Meserve, 1970: Selected level heights, temperatures and dew points for the Northern Hemisphere. NAVAIR 50-1C-52, [Available from Naval Weather Service Command, Washington, D. C.]

Godske, C. L., T. Bergeron, J. Bjerknes and R. C. Bundgaard, 1957: *Dynamic Meteorology and Weather Forecasting*. Amer. Meteor. Soc., 800 pp. (see Chap. 14).

Hora, S. L., 1952: Hora's Satpura hypothesis: an aspect of Indian biogeography. *Current Science, Bangalore*, **19**, 364–370.

Leith, C. E., 1973: The standard error of time-average estimates of climatic means. *J. Appl. Meteor.*, **12**, 1066–1069.

Lorenz, E. N., 1968: Climatic determinism. *Meteor. Monogr.*, No. 30, Amer. Meteor. Soc., 1–3.

Möller, F., 1951: Vierteljahrskarten des Niederschlags für die ganze Erde. *Petermanns Geographische Mitteilungen*, Justus Perthes, Gotha, 1–7.

Otterman, J., 1974: Baring high-albedo soils by over grazing: A hypothesized desertification method. *Science*, **186**, 531–533.

——, L. S. Walter and T. J. Schmugge, 1976: Observations from the ERTS imagery of overgrazing and cultivation impact on the Earth's surface. *Space Research XVI*, Akademie-Verlag, 15–21.

Rashke, E., T. H. Vonder Haar, W. R. Bandeen, M. Pasternak, 1973: The annual radiation balance of the earth-atmosphere system during 1969–70 from Nimbus 3 measurements. *J. Atmos. Sci.*, **30**, 341–364.

Ripley, E. A., 1976: Drought in the Sahara: Insufficient biogeophysical feedback? *Science*, **191**, p. 100.

Rockwood, A. A., and S. K. Cox, 1976: Satellite infrared surface albedo over Northwestern Africa. Atmos. Sci. Pap. No. 265, Colorado State University, 64 pp.

Schutz, C., and W. L. Gates, 1972: Global climatic data for surface, 800 mb, 400 mb: July. Rep. R-1029-ARPA, The Rand Corporation, Santa Monica.

SMIC Report, 1971: *Inadvertent Climate Modification*. The MIT Press, 308 pp.

Somerville, R. C. J., P. H. Stone, M. Halem, J. E. Hansen, J. S. Hogan, L. M. Druyan, G. Russell, A. A. Lacis, W. J. Quirk and J. Tenenbaum, 1974: The GISS model of the global atmosphere. *J. Atmos. Sci.*, **31**, 84–117.

Stern, M. E., 1954: Theory of the mean atmospheric perturbations produced by differential surface heating. *J. Meteor.*, **11**, 495–502.

Stone, P. H., S. Chow and W. J. Quirk, 1977: The July climate and a comparison of the January and July climates simulated by the GISS general circulation model. *Mon. Wea. Rev.*, **105**, 170–194.

Tanaka, M., B. C. Weare, A. R. Navato, and R. E. Newell, 1975: Recent African rainfall patterns. *Nature*, **255**, 201–203.

Thompson, B. W., 1965: *The Climate of Africa*. Oxford University Press, 132 pp.